Code equations

Yvonne Ban

7 August 2019

Contents

1 Empirical inputs

Input	Value	Confidence
wI, width of inductor	4×10^{-6} m	100%
lI, length of inductor	4×10^{-4} m	100%
tI, thickness of inductor	1.8×10^{-8} m	100%
Tc, critical temperature	1.4 K	100%
tau0, characteristic electron-phonon interaction time	4.38×10^{-7} s	0%
T, operating temperature	0.1 K	100%
R_nsp, normal sheet resistivity	90 Ohms/square	100%
lamb, wavelength of photons	1.1×10^{-3} m	100%
delta_nuopt, optical bandwidth	1×10^{10} Hz	90%
Lg, geometric inductance	3×10^{-9} H	100%
C, capacitor capacitance in circuit	5×10^{-12} F	100%
eta_opt, optical efficiency	0.8	100%
eta_pb, pair-breaking efficiency	0.57	100%
tau_phon_br, time for phonon to break Cooper pair	1×10^{-10} s	0%
Qc, coupling quality factor	5×10^{4}	100%
Ql, loss quality factor	2×10^{4}	90%
N0, single-spin density of electron states at Fermi energy[1]	8.277×10^{46} J^{-1}m^{-3}	90%
P_read, readout power[2]	6.31×10^{-12} W	0%
T_amp, amplifier noise temperature[3]	3 K	0%
deltav_read, readout bandwidth[4]	50 Hz	0%
V_read, readout voltage[5]	1.776×10^{-5} V	0%

Table 1: Empirical inputs

2 Constants

2.1 VI, volume of inductor

Input	Confidence
wI, width of inductor	100%
lI, length of inductor	100%
tI, thickness of inductor	100%

Table 2: Inputs to VI, volume of inductor

[1] Derived from value for TiN, from Shirokoff et al (2012)
[2] Currently unused
[3] Currently unused
[4] Currently unused
[5] Currently unused

$$V_I = w_I l_I t_I$$

2.2 nsq, number of squares of inductor

Input	Confidence
wI, width of inductor	100%
lI, length of inductor	100%

Table 3: Inputs to nsq, number of squares of inductor

$$n_{\text{sq}} = \frac{w_I}{l_I}$$

2.3 nu_opt, frequency of photons

Input	Confidence
lamb, wavelength of photons	100%

Table 4: Inputs to nu_opt, frequency of photons

$$\nu_{\text{opt}} = c\lambda$$

2.4 E_gamma, energy of photons

Input	Confidence
nu_opt, frequency of photons	100%

Table 5: Inputs to E_gamma, energy of photons

$$E_\gamma = h\nu_{\text{opt}}$$

2.5 delta0, gap energy at 0K

Flanigan p.20 and Jay

Input	Confidence
Tc, critical temperature	100%

Table 6: Inputs to delta0, gap energy at 0K

$$\Delta_0 = 1.764kT_c$$

2.6 delta, gap energy at T

Zmuidzinas eq.4, basically identical to delta0.

Input	Confidence
delta0, gap energy at 0K	100%

Table 7: Inputs to delta, gap energy at T

$$\Delta = \Delta_0 \left(1 - \sqrt{2\pi k \Delta_0} e^{\frac{\Delta_0}{kT}}\right)$$

2.7 sigma_n, normal conductivity just above Tc

Flanigan (private correspondence)

Input	Confidence
R_nsp, normal sheet resistivity	100%
tI, thickness of inductor	100%

Table 8: Inputs to sigma_n, normal conductivity just above Tc

$$\sigma_n = \frac{1}{R_{\text{nsq}} t_I}$$

2.8 lambL, (London) penetration depth in the thin film limit

Zmuidzinas eq.12 (currently unused)

Input	Confidence
sigma_n, normal conductivity just above Tc	50%
tI, thickness of inductor	100%

Table 9: Inputs to lambL, (London) penetration depth in the thin film limit

$$\lambda_L = \frac{\hbar}{\pi \mu_0 t_I \Delta \sigma_n}$$

2.9 N_qp_photon, number of quasiparticles produced per photon

Flanigan eq.3.67

Input	Confidence
eta_pb, pair-breaking efficiency	100%
nu_opt, frequency of photons	100%
delta, gap energy at T	100%

Table 10: Inputs to N_qp_photon, number of quasiparticles produced per photon

$$N_{\mathrm{qp,phot}} = \frac{h\eta_{\mathrm{pb}}\nu_{\mathrm{opt}}}{\Delta}$$

3 Intrinsic parameters (intrinsic to material)

3.1 R_qp, intrinsic quasiparticle recombination constant

Flanigan eq.3.14

Input	Confidence
delta0, gap energy at 0K	100%
N0, single-spin density of electron states at Fermi energy	90%
tau0, characteristic electron-phonon interaction time	0%

Table 11: Inputs to R_qp, intrinsic quasiparticle recombination constant

$$R_{\mathrm{qp}} = \frac{2\left(\frac{\Delta_0}{kT_c}\right)^3}{N_0\Delta_0\tau_0}$$

4 Thermal parameters (depend on T)

4.1 n_qp_therm, quasiparticle density due to thermal effects at T

Flanigan eq.3.10

Input	Confidence
delta0, gap energy at 0K	100%
N0, single-spin density of electron states at Fermi energy	90%
T, operating temperature	100%

Table 12: Inputs to n_qp_therm, quasiparticle density due to thermal effects at T

$$n_{\text{qp,therm}} = 2N_0\sqrt{2\pi kT\Delta_0}e^{-\frac{\Delta_0}{kT}}$$

4.2 gamma_G, low-temperature thermal generation rate at T

Flanigan eq.3.17

Input	Confidence
delta0, gap energy at 0K	100%
N0, single-spin density of electron states at Fermi energy	90%
tau0, characteristic electron-phonon interaction time	0%
T, operating temperature	100%
Tc, critical temperature	100%

Table 13: Inputs to gamma_G, low-temperature thermal generation rate at T

$$\gamma_G = \frac{16N_0\Delta_0^3\pi T}{\tau_0 k^2 T_c^3}e^{-\frac{2\Delta_0}{kT}}$$

5 Steady-state parameters

5.1 tau_phon_es, phonon escape time

Flanigan eq.3.19 (currently unused)

Input	Confidence
tI, thickness of inductor	100%
eta_phon_trans, transmission probability per encounter	0%
s, probably speed of sound	0%

Table 14: Inputs to tau_phon_es, phonon escape time

$$\begin{aligned}\tau_{\text{phon,es}} &= \frac{4t_I}{s\eta_{\text{phon, es}}}\\ \eta_{\text{phon,es}} &= 1\times10^{-9}\\ s &= 6.4\times10^{3}\,\text{ms}^{-1}\end{aligned}$$

5.2 F_phon, phonon trapping factor

Flanigan eq.3.20 (currently unused)

Input	Confidence
tau_phon_br, time for phonon to break Cooper pair	0%
tau_phon_es, phonon escape time	0%

Table 15: Inputs to F_phon, phonon trapping factor

$$F_{\text{phon}} = 1 + \frac{\tau_{\text{phon,es}}}{\tau_{\text{phon,br}}}$$

5.3 R_eff, effective quasiparticle recombination constant

Flanigan p.31 (currently ignores F_phon)

Input	Confidence
R_qp, intrinsic quasiparticle recombination constant	0%
F_phon, phonon trapping factor	0%

Table 16: Inputs to R_eff, effective quasiparticle recombination constant

$$R_{\text{eff}} = \frac{R_{\text{qp}}}{F_{\text{phon}}}$$

5.4 tau_qp, quasiparticle relaxation time

Flanigan p.46 (currently unused)

Input	Confidence
R_eff, effective quasiparticle recombination constant	0%
gamma_G, low-temperature thermal generation rate at T	0%

Table 17: Inputs to tau_qp, quasiparticle relaxation time

$$\tau_{\text{qp}} = \frac{1}{\sqrt{4R_{\text{eff}}\gamma_G}}$$

5.5 n_qp_ss, steady-state quasiparticle density

Flanigan p.43. Should match nqp0, assuming ignoring F_phon. tau0 term cancels out from R_eff and gamma_G.

Input	Confidence
R_eff, effective quasiparticle recombination constant	0%
gamma_G, low-temperature thermal generation rate at T	0%

Table 18: Inputs to n_qp_ss, steady-state quasiparticle density

$$n_{\text{qp,ss}} = \sqrt{\frac{\gamma_G}{R_{\text{eff}}}}$$

5.6 N_qp_ss, steady-state quasiparticle number in resonator

Flanigan p.57. tau0 term cancels out from R_eff and gamma_G.

Input	Confidence
R_eff, effective quasiparticle recombination constant	0%
gamma_G, low-temperature thermal generation rate at T	0%
VI, volume of inductor	100%

Table 19: Inputs to N_qp_ss, steady-state quasiparticle number in resonator

$$N_{\text{qp,ss}} = V_I\sqrt{\frac{\gamma_G}{R_{\text{eff}}}}$$

6 Optical generation

6.1 Gamma_opt, constant optical power quasiparticle generation rate

Flanigan eq.3.68. N.B: CODE CURRENTLY DOES NOT USE dGamma_dP AS IT ASSUMES OPTICAL EFFICIENCY ACCOUNTED FOR.

Input	Confidence
P_opt, incident optical power	100%
dGamma_dP, responsivity of quasiparticle generation rate to optical power[6]	100%
eta_pb, pair-breaking efficiency	100%
delta, gap energy at T	100%

Table 20: Inputs to Gamma_opt, constant optical power quasiparticle generation rate

$$\Gamma_{\text{opt}} = \frac{dP_{\text{abs}}}{dP_{\text{inc}}} \frac{P_{\text{opt}}\eta_{\text{pb}}}{\Delta}$$

7 All together now

7.1 N_qp_tot, total number of quasiparticles in resonator due to thermal and constant optical power effects

Flanigan p.57. tau0 term cancels out between R_eff and gamma_G, but not between R_eff and Gamma_opt. Effects are transmitted forward to fnew and Q_qp.

Input	Confidence
P_opt, incident optical power	100%
Gamma_opt, constant optical power quasiparticle generation rate	100%
R_eff, effective quasiparticle recombination constant	0%
gamma_G, low-temperature thermal generation rate at T	0%
VI, volume of inductor	100%

Table 21: Inputs to N_qp_tot, total number of quasiparticles in resonator due to thermal and constant optical power effects

$$N_{\text{qp,tot}} = \sqrt{\frac{V_I^2\gamma_G + V_I\Gamma_{\text{opt}}(P_{\text{opt}})}{R_{\text{eff}}}}$$

8 Complex conductivity

8.1 sigma1_0, real part of complex conductivity at T=0K

Flanigan p.35

[6] Currently unused

Input	Confidence

Table 22: Inputs to sigma1_0, real part of complex conductivity at T=0K

$$\sigma_1(0) = 0$$

8.2 sigma2_0, imag part of complex conductivity at T=0K

Flanigan p.35

Input	Confidence
sigma_n, normal conductivity just above Tc	100%
delta0, gap energy at 0K	100%
f, readout frequency	100%

Table 23: Inputs to sigma2_0, imag part of complex conductivity at T=0K

$$\sigma_2(0) = \frac{\pi \Delta_0 \sigma_n}{hf}$$

8.3 sigma1rat, ratio of real part of complex conductivity to quasiparticle density response at T

Flanigan eq.3.79. Used in dsig1_dN.

Input	Confidence
delta0, gap energy at 0K	100%
f, readout frequency	100%
T, operating temperature	100%

Table 24: Inputs to sigma1rat, ratio of real part of complex conductivity to quasiparticle density response at T

$$\Upsilon_{\sigma_1}(f) = \sqrt{\frac{8\Delta_0}{\pi^3 kT}} \sinh \frac{hf}{2kT} K_0 \left(\frac{hf}{2kT} \right)$$

8.4 sigma2rat, ratio of imag part of complex conductivity to quasiparticle density response at T

Flanigan eq.3.80. Used in dsig2_dN.

Input	Confidence
delta0, gap energy at 0K	100%
f, readout frequency	100%
T, operating temperature	100%

Table 25: Inputs to sigma2rat, ratio of imag part of complex conductivity to quasiparticle density response at T

$$\Upsilon_{\sigma_2}(f) = -1 - \sqrt{\frac{2\Delta_0}{\pi k T}} e^{-\frac{hf}{2kT}} I_0\left(\frac{hf}{2kT}\right)$$

8.5 sigma1, real part of complex conductivity at T

Uses dsig1_dN.

Input	Confidence
P_opt, incident optical power	100%
N_qp_tot, total number of quasiparticles in resonator	90%
sigma1_0, real part of complex conductivity at T=0K	100%
dsig1_dN, responsivity of sigma1 against N_qp_tot	100%
f, readout frequency	100%

Table 26: Inputs to sigma1, real part of complex conductivity at T

$$\sigma_1(f) = N_{\mathrm{qp,tot}}(P_{\mathrm{opt}})\frac{d\sigma_1(f)}{dN_{\mathrm{qp}}} + \sigma_1(0)$$

8.6 sigma2, imag part of complex conductivity at T

Uses dsig2_dN.

Input	Confidence
P_opt, incident optical power	100%
N_qp_tot, total number of quasiparticles in resonator	90%
sigma2_0, imag part of complex conductivity at T=0K	100%
dsig2_dN, responsivity of sigma2 against N_qp_tot	100%
f, readout frequency	100%

Table 27: Inputs to sigma2, imag part of complex conductivity at T

$$\sigma_2(f) = N_{\text{qp,tot}}(P_{\text{opt}}) \frac{d\sigma_2(f)}{dN_{\text{qp}}} + \sigma_2(f, 0)$$

8.7 sigma, complex conductivity at T

Flanigan p.34

Input	Confidence
P_opt, incident optical power	100%
sigma1, real part of complex conductivity at T	90%
sigma2, imag part of complex conductivity at T	90%
f, readout frequency	100%

Table 28: Inputs to sigma, complex conductivity at T

$$\sigma(f) = \sigma_1(f, P_{\text{opt}}) - i\sigma_2(f, P_{\text{opt}})$$

9 Surface impedance, reactance, (kinetic) inductance, resistance

9.1 Zs_0, surface impedance in thin film local limit at T=0K

Flanigan eq.3.35

Input	Confidence
sigma2_0, imag part of complex conductivity at T=0K	100%
tI, thickness of inductor	100%
f, readout frequency	100%

Table 29: Inputs to Zs_0, surface impedance in thin film local limit at T=0K

$$Z_s(f,0) = \frac{i}{t_I \sigma_2(f,0)}$$

9.2 Zs, surface impedance in thin film local limit at T

Flanigan eq.3.35

Input	Confidence
P_opt, incident optical power	100%
sigma, complex conductivity at T	90%
tI, thickness of inductor	100%
f, readout frequency	100%

Table 30: Inputs to Zs, surface impedance in thin film local limit at T

$$Z_s(f) = \frac{1}{t_I \sigma(f, P_{\text{opt}})}$$

9.3 Xs_0, surface reactance in thin film local limit at T=0K

Flanigan p.36

Input	Confidence
Zs_0, surface impedance in thin film local limit at T=0K	100%
f, readout frequency	100%

Table 31: Inputs to Xs_0, surface reactance in thin film local limit at T=0K

$$X_s(f,0) = \Im(Z_s(f,0))$$

9.4 Xs, surface reactance in thin film local limit at T

Flanigan p.36

Input	Confidence
P_opt, incident optical power	100%
Zs, surface impedance in thin film local limit at T	90%
f, readout frequency	100%

Table 32: Inputs to Xs, surface reactance in thin film local limit at T

$$X_s(f) = \Im(Z_s(f, P_{\text{opt}}))$$

9.5 Rs, surface resistance in thin film local limit at T

Flanigan p.36

Input	Confidence
P_opt, incident optical power	100%
Zs, surface impedance in thin film local limit at T	90%
f, readout frequency	100%

Table 33: Inputs to Rs, surface resistance in thin film local limit at T

$$R_s(f) = \Re(Z_s(f, P_{\text{opt}}))$$

9.6 Lk_0, kinetic inductance in thin film local limit at T=0K

Flanigan p.36

Input	Confidence
nsq, number of squares of inductor	100%
tI, thickness of inductor	100%
delta0, gap energy at 0K	100%
sigma_n, normal conductivity just above Tc	100%

Table 34: Inputs to Lk_0, kinetic inductance in thin film local limit at T=0K

$$L_k(0) = \frac{n_{\text{sq}} h}{2\pi^2 t_I \Delta_0 \sigma_n}$$

9.7 Lk, kinetic inductance in thin film local limit at T

Flanigan p.36

Input	Confidence
P_opt, incident optical power	100%
tI, thickness of inductor	100%
delta0, gap energy at 0K	100%
sigma_n, normal conductivity just above Tc	100%
N0, single-spin density of electron states at Fermi energy	90%
VI, volume of inductor	100%
sigma2rat, ratio of real part of complex conductivity to quasiparticle density response at T	100%

Table 35: Inputs to Lk, kinetic inductance in thin film local limit at T

$$L_k = L_k(0)\left(1 - \frac{N_{\mathrm{qp,tot}}(P_{\mathrm{opt}})\Upsilon_{\sigma_2}(f)}{2N_0\Delta_0 V_I + N_{\mathrm{qp,tot}}(P_{\mathrm{opt}})\Upsilon_{\sigma_2}(f)}\right)$$

10 Resonant frequency

10.1 alpha, effective kinetic inductance fraction in thin film local limit

Flanigan eq.3.62

Input	Confidence
Lk_0, kinetic inductance in thin film local limit at T=0K	100%
Lg, geometric inductance	100%

Table 36: Inputs to alpha, effective kinetic inductance fraction in thin film local limit

$$\alpha = \frac{L_k(0)}{L_g + L_k(0)}$$

10.2 f0, resonant frequency of resonator circuit at T=0K

Flanigan p.52

Input	Confidence
Lk_0, kinetic inductance in thin film local limit at T=0K	100%
Lg, geometric inductance	100%
C, capacitor capacitance in circuit	100%

Table 37: Inputs to f0, resonant frequency of resonator circuit at T=0K

$$f_0 = \frac{1}{2\pi\sqrt{C(L_g + L_k(0))}}$$

10.3 ffrac, fractional frequency shift in resonant frequency of circuit

Flanigan eq.3.63

Input	Confidence
alpha, effective kinetic inductance fraction in thin film local limit	100%
P_opt, incident optical power	100%
Lk, kinetic inductance in thin film local limit at T	90%
Lk_0, kinetic inductance in thin film local limit at T=0K	100%

Table 38: Inputs to ffrac, fractional frequency shift in resonant frequency of circuit

$$s = \frac{\alpha}{2}\frac{L_k(f, P_{\rm opt}) - L_k(0)}{L_k(0)}$$

10.4 fnew, resonant frequency of resonator circuit in thin film local limit

Flanigan eq.3.61

Input	Confidence
P_opt, incident optical power	100%
f0, resonant frequency of resonator circuit at T=0K	100%
ffrac, fractional frequency shift in resonant frequency of circuit	90%

Table 39: Inputs to fnew, resonant frequency of resonator circuit in thin film local limit

$$f_{\rm new} = f_0(1 - s(f, P_{\rm opt}))$$

10.5 fdet, detuning of resonant frequency from readout frequency

Flanigan p.50

Input	Confidence
P_opt, incident optical power	100%
f, readout frequency	100%
fnew, resonant frequency of resonator circuit in thin film local limit	90%

Table 40: Inputs to fdet, detuning of resonant frequency from readout frequency

$$x = \frac{f}{f_{\text{new}}(f, P_{\text{opt}})} - 1$$

11 Quality factors

11.1 Q_qp, quality factor of resonator circuit from quasiparticles

Flanigan eq.3.64

Input	Confidence
alpha, effective kinetic inductance fraction in thin film local limit	100%
P_opt, incident optical power	100%
Xs_0, surface reactance in thin film local limit at T=0K	100%
Rs, surface resistance in thin film local limit at T	90%
f, readout frequency	100%

Table 41: Inputs to Q_qp, quality factor of resonator circuit from quasiparticles

$$Q_{\text{qp}}(f) = \frac{X_s(f, 0)}{\alpha R_s(f, P_{\text{opt}})}$$

11.2 Qr, quality factor of resonator circuit in thin film local limit

Flanigan eq.3.58. Assumes internal quality factor Q_i is dominated by Q_qp.

Input	Confidence
P_opt, incident optical power	100%
Q_qp, quality factor of resonator circuit from quasiparticles	90%
Qc, coupling quality factor	100%
Ql, loss quality factor	90%
f, readout frequency	100%

Table 42: Inputs to Qr, quality factor of resonator circuit in thin film local limit

$$Q_\mathrm{r} = \left(\frac{1}{Q_c} + \frac{1}{Q_l} + \frac{1}{Q_\mathrm{qp}(f, P_\mathrm{opt})}\right)^{-1}$$

12 Responsivities

12.1 dPabs_dPinc, responsivity of absorbed optical power to incident optical power

Flanigan eq.3.66

Input	Confidence
eta_opt, optical efficiency	100%

Table 43: Inputs to dPabs_dPinc, responsivity of absorbed optical power to incident optical power

$$\frac{dP_\mathrm{abs}}{dP_\mathrm{inc}} = \eta_\mathrm{opt}$$

12.2 dGamma_dP, responsivity of quasiparticle generation rate to optical power

Flanigan eq.3.69

Input	Confidence
eta_pb, pair-breaking efficiency	100%
delta0, gap energy at 0K	100%

Table 44: Inputs to dGamma_dP, responsivity of quasiparticle generation rate to optical power

$$\frac{d\Gamma_\mathrm{opt}}{dP_\mathrm{opt}} = \frac{\eta_\mathrm{pb}}{\Delta_0}$$

12.3 dN_qp_tot_dGamma, responsivity of N_qp_tot to quasiparticle generation rate

Flanigan eq.3.72

Input	Confidence
P_opt, incident optical power	100%
Gamma_opt, constant optical power quasiparticle generation rate	100%
R_eff, effective quasiparticle recombination constant	0%
gamma_G, low-temperature thermal generation rate at T	0%
VI, volume of inductor	100%

Table 45: Inputs to dN_qp_tot_dGamma, responsivity of N_qp_tot to quasiparticle generation rate

$$\frac{dN_{\text{qp,tot}}}{d\gamma} = \frac{1}{2}\sqrt{\frac{1}{R_{\text{eff}}(\gamma_G + \frac{\Gamma_{\text{opt}}(P_{\text{opt}})}{V_I})}}$$

12.4 dsig1_dN, responsivity of sigma1 to N_qp_tot

Flanigan eq.3.81. Uses sigma1rat and used in calculation of sigma1.

Input	Confidence
sigma2_0, imag part of complex conductivity at T=0K	100%
sigma1rat, ratio of real part of complex conductivity to quasiparticle density response at T	100%
N0, single-spin density of electron states at Fermi energy	100%
delta0, gap energy at 0K	100%
VI, volume of inductor	100%
f, readout frequency	100%

Table 46: Inputs to dsig1_dN, responsivity of sigma1 to N_qp_tot

$$\frac{d\sigma_1(f)}{dN_{\text{qp,tot}}} = \frac{\sigma_2(f,0)\Upsilon_{\sigma_1}(f)}{2N_0\Delta_0 V_I}$$

12.5 dsig2_dN, responsivity of sigma2 to N_qp_tot

Flanigan eq.3.82. Uses sigma2rat and used in calculation of sigma2.

Input	Confidence
sigma2_0, imag part of complex conductivity at T=0K	100%
sigma2rat, ratio of real part of complex conductivity to quasiparticle density response at T	100%
N0, single-spin density of electron states at Fermi energy	100%
delta0, gap energy at 0K	100%
VI, volume of inductor	100%
f, readout frequency	100%

Table 47: Inputs to dsig2_dN, responsivity of sigma2 to N_qp_tot

$$\frac{d\sigma_2(f)}{dN_{\mathrm{qp,tot}}} = \frac{\sigma_2(f,0)\Upsilon_{\sigma_2}(f)}{2N_0\Delta_0 V_I}$$

12.6 dRs_dsig1, responsivity of surface resistance Rs to sigma1

Flanigan eq.3.83

Input	Confidence
Xs_0, surface reactance in thin film local limit at T=0K	100%
sigma2_0, imag part of complex conductivity at T=0K	100%
f, readout frequency	100%

Table 48: Inputs to dRs_dsig1, responsivity of surface resistance Rs to sigma1

$$\frac{dR_s(f)}{d\sigma_1} = \frac{X_s(f,0)}{\sigma_2(f,0)}$$

12.7 dXs_dsig2, responsivity of surface reactance Xs to sigma2

Flanigan eq.3.84

Input	Confidence
Xs_0, surface reactance in thin film local limit at T=0K	100%
sigma2_0, imag part of complex conductivity at T=0K	100%
f, readout frequency	100%

Table 49: Inputs to dXs_dsig2, responsivity of surface reactance Xs to sigma2

$$\frac{dX_s(f)}{d\sigma_2} = -\frac{X_s(f,0)}{\sigma_2(f,0)}$$

12.8 dlambqp_dRs, responsivity of quasiparticle loss factor lambda_qp to surface resistance Rs

Flanigan eq.3.87

Input	Confidence
alpha, effective kinetic inductance fraction in thin film local limit	100%
P_opt, incident optical power	100%
Xs_0, surface reactance in thin film local limit at T=0K	100%
f, readout frequency	100%

Table 50: Inputs to dlambqp_dRs, responsivity of quasiparticle loss factor lambda_qp to surface resistance Rs

$$\frac{d\lambda_{\mathrm{qp}}}{dR_s(f)} = \frac{\alpha(P_{\mathrm{opt}})}{X_s(f,0)}$$

12.9 dx_dXs, responsivity of frequency detuning x to surface reactance Xs

Flanigan eq.3.88

Input	Confidence
alpha, effective kinetic inductance fraction in thin film local limit	100%
P_opt, incident optical power	100%
Xs_0, surface reactance in thin film local limit at T=0K	100%
f, readout frequency	100%

Table 51: Inputs to dx_dXs, responsivity of frequency detuning x to surface reactance Xs

$$\frac{dx}{dX_s(f)} = \frac{\alpha(P_{\mathrm{opt}})}{2X_s(f,0)}$$

12.10 dQqp_dRs, responsivity of quasiparticle quality factor Q_qp to surface resistance Rs

Input	Confidence
alpha, effective kinetic inductance fraction in thin film local limit	100%
P_opt, incident optical power	100%
Q_qp, quality factor of resonator circuit from quasiparticles	100%
Xs_0, surface reactance in thin film local limit at T=0K	100%
f, readout frequency	100%

Table 52: Inputs to dQqp_dRs, responsivity of quasiparticle quality factor Q_qp to surface resistance Rs

$$\frac{dQ_{\mathrm{qp}}(f)}{dR_s(f)} = -\frac{Q_{\mathrm{qp}}(f)^2\alpha(P_{\mathrm{opt}})}{X_s(f,0)}$$

13 S21

13.1 S21, resonator quality factor of resonator circuit in thin film local limit

Flanigan eq.3.60

Input	Confidence
P_opt, incident optical power	100%
f, readout frequency	100%
Q_r, quality factor of resonator circuit in thin film local limit	90%
Qc, coupling quality factor	100%
fdet, detuning of resonant frequency from readout frequency	90%
A, symmetry factor	90%

Table 53: Inputs to S21, resonator quality factor of resonator circuit in thin film local limit

$$S_{21} = 1 - \frac{Q_r(f, P_{\mathrm{opt}})(1+iA)}{Q_c(1+2iQ_r(f,P_{\mathrm{opt}})x(f,P_{\mathrm{opt}}))}$$

14 NEP

14.1 nep_phot, noise equivalent power (NEP) of photon noise

Flanigan eq.5.5, from shot noise and wave noise

Input	Confidence
P_opt, incident optical power	100%
nu_opt, frequency of photons	100%
delta_nuopt, optical bandwidth	90%

Table 54: Inputs to nep_phot, noise equivalent power (NEP) of photon noise

$$\mathrm{NEP}(P_{\mathrm{opt}}) = \sqrt{2\left(h\nu P_{\mathrm{opt}} + \frac{P_{\mathrm{opt}}^2}{\Delta\nu}\right)}$$

14.2 nep_rec, noise equivalent power (NEP) of recombination noise due to P_opt

Flanigan eq.5.19

Input	Confidence
P_opt, incident optical power	100%
delta0, gap energy at 0K	100%
eta_opt, optical efficiency	100%
eta_pb, pair-breaking efficiency	100%

Table 55: Inputs to nep_rec, noise equivalent power (NEP) of recombination noise due to P_opt

$$\mathrm{NEP}(P_{\mathrm{opt}}) = 2\sqrt{\frac{\Delta_0 P_{\mathrm{opt}}}{\eta_{\mathrm{opt}}\eta_{\mathrm{pb}}}}$$

15 Finding P_opt

15.1 P_opt_r, P_opt value from fnew

Input	Confidence
fnew, resonant frequency of resonator circuit	100%

Table 56: Inputs to P_opt_r, P_opt value from fnew

$$L_k(P_{\text{opt}}) = 2(L_g + L_k(T=0))(1 - 2\pi f_{\text{new}}\sqrt{C(L_g + L_k(T=0))}) + L_g$$

$$N_{\text{qp,tot}} = -\frac{2N_0\Delta_0 V_I}{\Upsilon_{\sigma_2}(f)}\left(1 + \frac{L_k(T=0)}{L_k(P_{\text{opt}})}\right)$$

$$P_{\text{opt}} = \frac{\Delta}{\eta_{\text{pb}}\eta_{\text{opt}}}\left(\frac{N^2_{\text{qp,tot}}R_{\text{eff}}}{V_I} - \gamma_G\right)$$

16 What doesn't work yet

16.1 f0 resonance frequency

With parameters meant to have fnew(0)=500 MHz, i.e. nqp0=10^{20} and R_nsq=90 Ω, and tau0 set at value for Al (4.38×10^{-7} s), actual fnew(0)=1.281 GHz. Linked to R_nsq.

16.2 ffrac too low

Fig. 1: With parameters set to have fnew(0)=500 kHz, i.e. nqp0=10^{20} and R_nsq=$1.7536 \times 10^4\,\Omega$, and tau0 set at value for Al (4.38×10^{-7} s), ffrac changes very little with P_opt. Linked to nqp0.

Fig. 2 and Fig. 3: With only change from default being tau0=10 s, ffrac follows empirical trend.

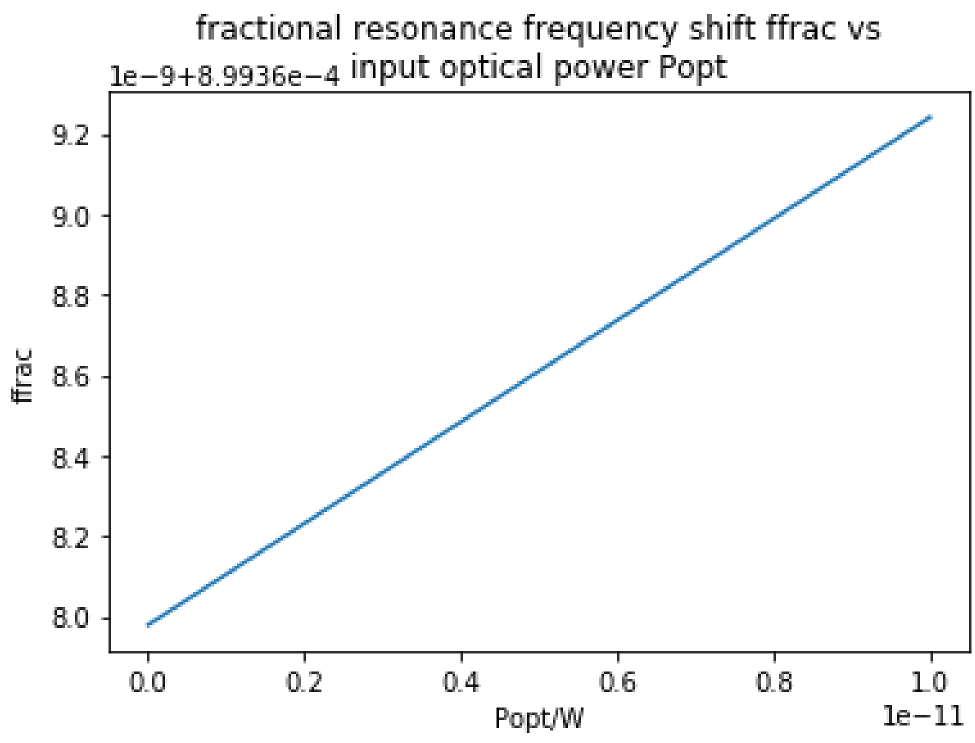

Figure 1: Fractional frequency shift with R_nsq=$1.7536 \times 10^4\,\Omega$ so fnew(0)=500 kHz.

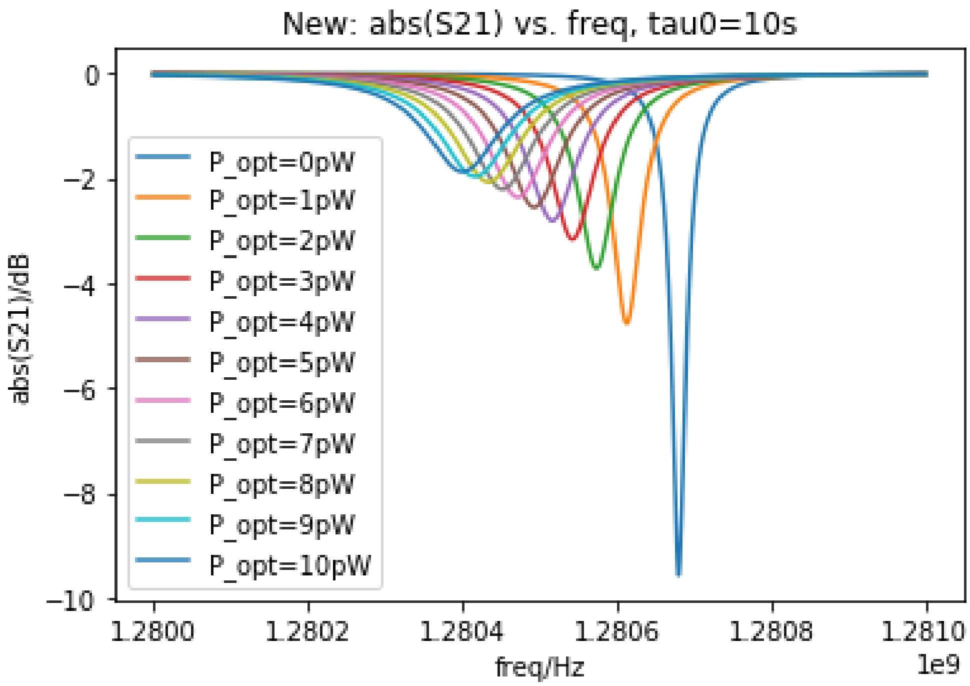

Figure 2: Resonance curves with only tau0 changed from 4.38×10^{-7} s to 10 s.

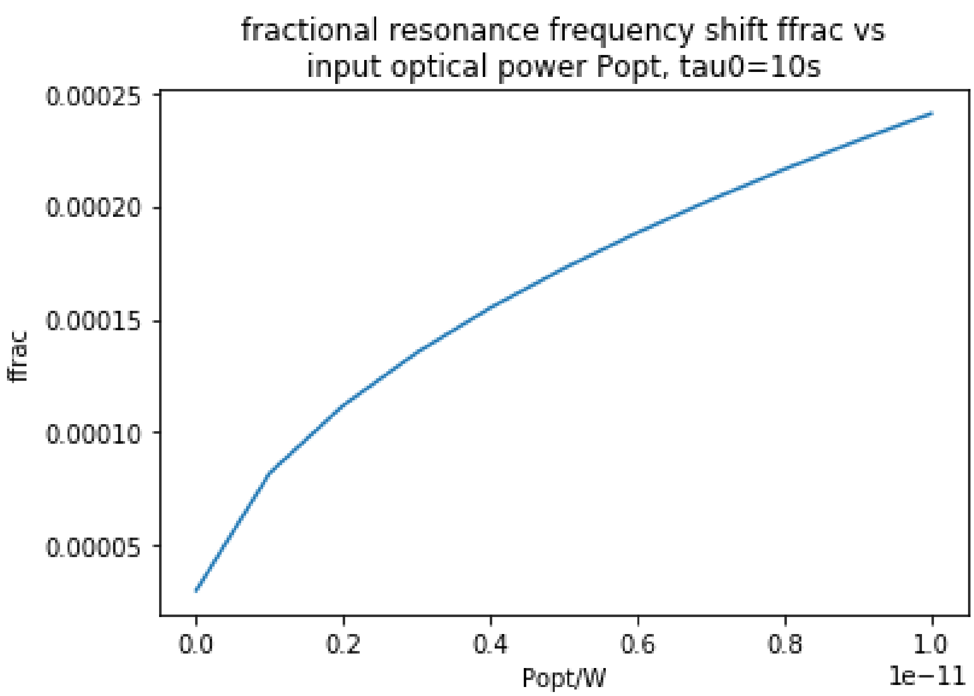

Figure 3: Fractional frequency shift with only tau0 changed from 4.38×10^{-7} s to 10 s.

16.3 Qr too low or drops too quickly

Fig. 4: With parameters set to have fnew(0)=500 kHz and tau0 set at value for Al (4.38×10^{-7} s), Qr too low or drops too quickly with P_opt. Linked to nqp0.

Fig. 5: With only change from default being tau0=10 s, Qr follows empirical trend.

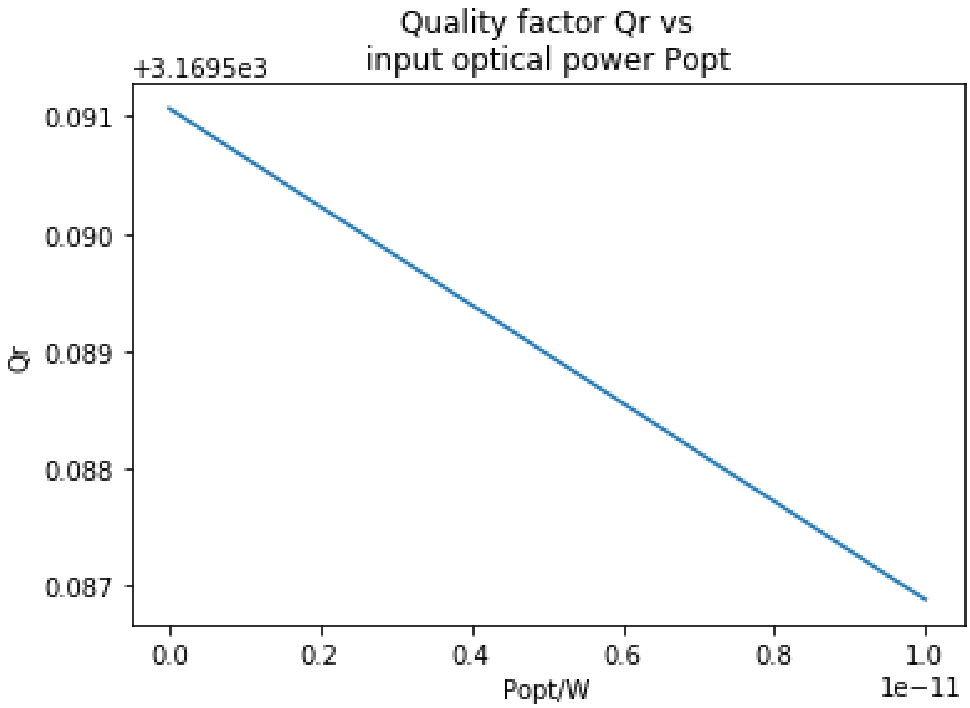

Figure 4: Quality factor with R_nsq=$1.7536 \times 10^4\,\Omega$ so fnew(0)=500 kHz.

16.4 Singularity in L_k (RESOLVED)

There is a singularity in L_k as a function of temperature T that affects resonance frequency fnew as shown in Fig. 6. It can be traced to the L_k denominator term $(2N_0\Delta_0V_I + N_{\mathrm{qp,tot}}(P_{\mathrm{opt}})\Upsilon_{\sigma_2})$. The term sigma2rat, Υ_{σ_2}, is negative, while the other terms are positive. This causes a zero to appear in the denominator for a certain value of T, causing the resonance frequency to blow up, which is obviously not physical. However, it's fine because the singularity is way above T_c.

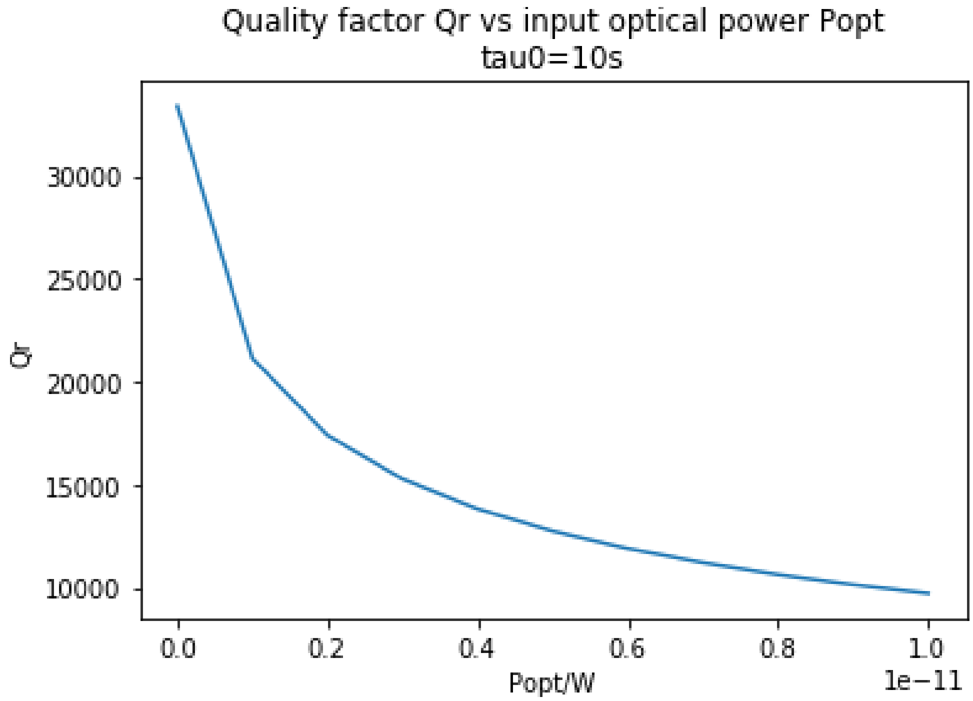

Figure 5: Quality factor with only tau0 changed from 4.38×10^{-7} s to 10 s.

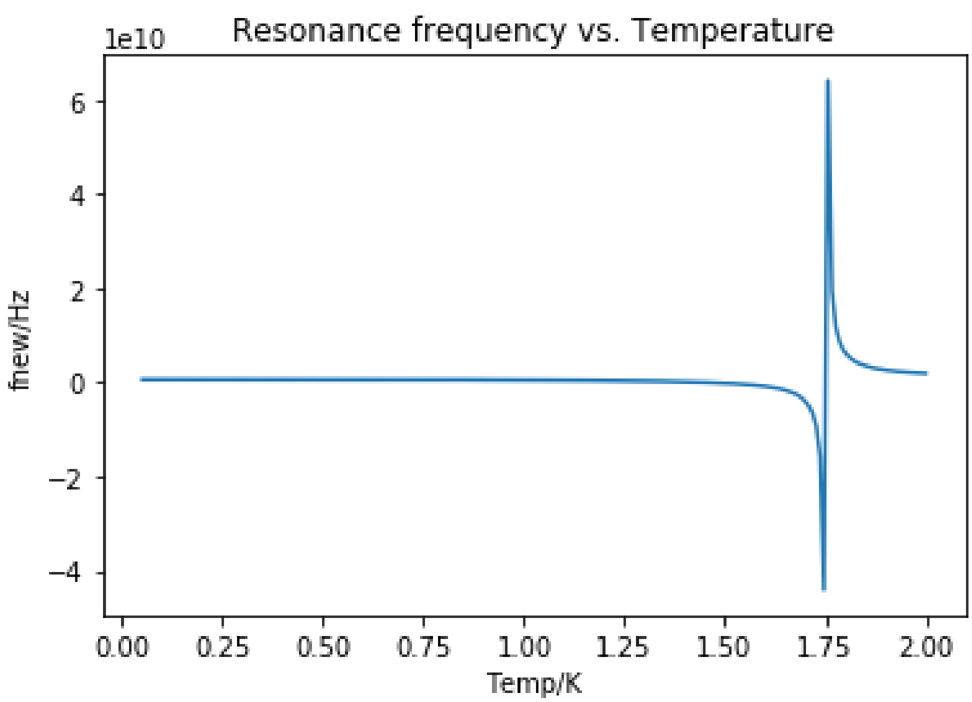

Figure 6: Singularity in resonance frequency as a function of temperature.